

USE OF A LARGE-SCALE SPATIAL COHERENCE OF TURBULENCE PATTERNS FOR PREDICTING OBSERVATION CONDITIONS AT ASTRONOMICAL OBSERVATORIES

Marc S. Sarazin

European Southern Observatory (ESO), Munich
Received September 29, 1992

The quality of vision and scintillations have been simultaneously recorded with identical instrumentation during several nights at two astronomical observatories in Chile (Las Campanas and La Silla) located along the prevailing wind direction some ten kilometers apart. High correlation between the observed signals has shown that the atmospheric turbulence keeps its structure at a long distance.

Based on this studied property of the atmospheric turbulence it is possible to make a short-term (for several hours) forecast of the visibility conditions for the ground-based observatories. Such a forecasting can be very useful when making a timetable for observations with a modern ground-based telescope.

This problem is now being studied at the South European Observatory as part of the programme on development of the Astronomic Weather Station for the Very Big Telescope (VBT).

1. THE ASTRONOMICAL WEATHER STATION FOR THE VERY BIG TELESCOPE

The Astronomical Weather Station (AWS) is the future interface between the observer and the terrestrial environment of the VBT observatory. Its function is to improve the quality of observations and to provide for an efficient use of the telescope time. It must provide the remote observer with the appropriate environmental data, and eventually replace him for a part of the decision making process. It must have three basic functions which will be described below in more detail. The functions are sensing, modeling, and advising.

1. The sensing unit includes all meteorological and atmospheric local sensors with their interfaces connected with a computer. A communication link with the outer world also makes it possible to collect data from remote sensors, i.e., data from satellites, radiosondes, professional synoptic bulletins, and the like.

2. The modelling unit filters the input information and produces an accurate picture of the current environmental state. It can also form the short-term predictions when prediction models are available.¹

3. The User Interface is an expert system with several levels of capabilities which are, by an order of complexity, the following:

a) display of information about current conditions as well as of archived data accessible from the telescopes, remote control center in Garching, and astronomical institutes in the programme Member States;

b) determination of optimal instrumental setup to help the astronomers to conduct their observations with the particular environmental constraints imposed on the telescope (for example, wind load, and local vision conditions) and on the instrument (for example, the optimal exposure time for image recording and add-up techniques),

c) determination of an optimal schedule of observations, e.g., to be able to benefit of the optimal atmospheric conditions when they occur,

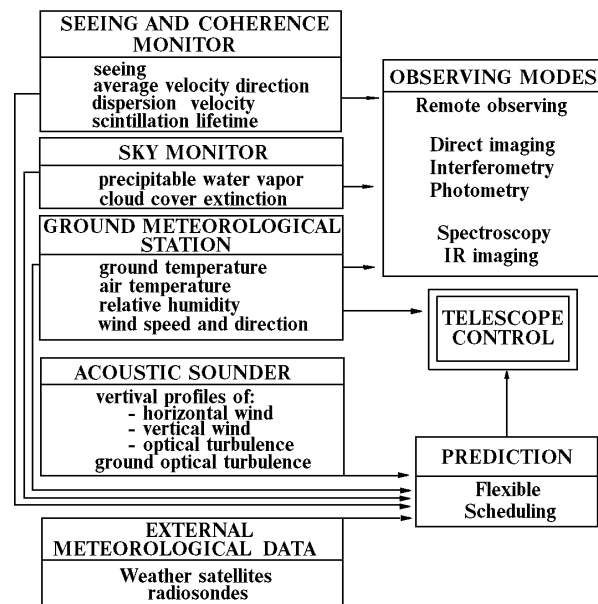


FIG. 1. The VBT astronomical weather station.

d) direct control of some telescope functions, which are, e.g., the thermal control of the enclosures, the thermal control of light paths based on predictions of air temperature for the next night or hour.²

2. LOCAL SPATIAL CORRELATION OF SEEING AND SCINTILLATION QUALITY

2.1. Scope of the study. Within the framework of the site evaluation for the VBT, it appeared to be of interest for the Site Selection Working Group to compare one of the potentially suitable site at the existing observatory in Northern Chile with the other one in La

Silla.³ The observatory of Las Campanas was chosen, where a similar analysis was conducted by the Carnegie Institute in view of the construction of an eight meter class telescope. Thanks to the good will and cooperation of local administrations, it was possible to run simultaneously several instruments at both sites during 14 nights successively, from November 27 till December 10, 1989.

2.2. Description of the observation sites. The observatory of Las Campanas is arranged at several peaks along a large ridge approximately facing the prevailing North winds, standing well above the surrounding terrain. Our test point was in the western part of the observatory, close to the Dupont telescope at an altitude of 2280 m.

The other test point was in Cerro Vizcachas located 7 km to the eastern end of the La Silla ridge. The Vizcachas/La Silla ridge stands at 2400 m altitude above the sea level, 30 km to the south of Las Campanas, separated from it by a rather perturbed landscape with several mountain ridges of the same altitude and 1000 m deep canyons.

2.3. Instrumentation. The campaign lasted 14 nights during which various instruments were simultaneously operated at both observation points:

a) Vizcachas—La Silla: A differential image motion monitor (DIMM2) described in Ref. 4 at Vizcachas is mounted on a 5 m high platform, near the windward slope (see Fig. 2).

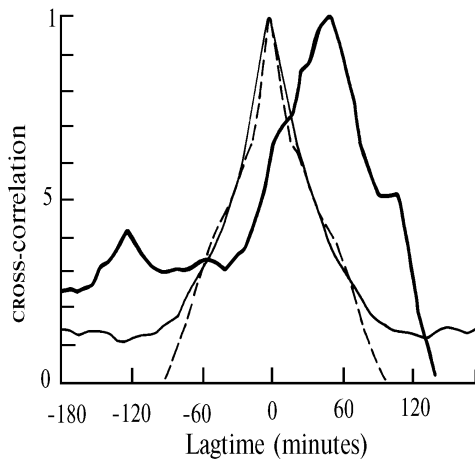


FIG. 2. The temporal correlation of vision quality measurements (the measured interval is 500 sec.): Vizcachas autocorrelation (dashed line), Campanas autocorrelation (dotted line), and cross-correlation (solid line).

It allows one to estimate the vision quality every two minutes; wind speed is also recorded online. An acoustic sounder (SODAR) is located at the northern side of the observation tower basement, 10 m under the vision monitor.

b) Las Campanas: A mobile differential image motion monitor (DIMM3), identical to DIMM2, is mounted on a 2 m high platform at the northern slope of the peak. Wind velocity at the ground level is recorded in online regime.

Each DIMM is also equipped with a scintillometer of 3 cm diameter aperture and 1 kHz bandpass, looking at the same star.

3. ANALYSIS OF TEMPORAL CORRELATION

3.1. Vision. Quality of vision is defined as the full width at half maximum (FWHM) of a long exposure image obtained at the focus of a large telescope taking into account limitations imposed by the atmosphere:

$$FWHM = 0.976 \frac{1}{r_0} = 5.345 \lambda^{-1/5} \left[(\cos \gamma)^{-1} \int C_n^2(z) dz \right]^{3/5}, \quad (1)$$

where C_n^2 is the structural function of the atmospheric index of refraction, r_0 is the aperture radius, and λ is the wavelength.

At $\lambda = 0.5$ mm, and in units of arc sec, this becomes

$$FWHM = 2.0 \cdot 10^7 \left[\int C_n^2(z) dz \right]^{3/5}. \quad (2)$$

In the theory of atmospheric turbulence one often uses the hypothesis that the turbulence moves with wind without modification of its statistical properties along the path (frozen turbulence). Determination of the average velocities of the turbulence layers⁵ and their variances is of interest for optimizing interferometric observational techniques.

Since the two test sites are 27 km apart from each other along the direction to the north, this data set is used to show that a portion of the turbulence detected at Las Campanas is transported without much changes to Vizcachas.

Figure 2 shows that the normalized temporal cross-correlation between the two time series of observations has a pronounced peak at a 50 min delay of the Vizcachas measurements with respect to the Las Campanas ones. The autocorrelation functions of the vision at the two sites shown in the same figure determine the time constant of the atmosphere. The broadening of the cross-correlation peak corresponds to the dispersion of the wind velocity around the average value of 9 m/s. The level of the cross-correlation peak corresponds to 40% of the product of the rms quality of vision at the sites.

3.2. Scintillations. The index of scintillation is defined as:

$$\sigma_I^2 = 19.12 \lambda^{-7/6} (\cos \gamma)^{-11/6} \int_0^\infty C_n^2(z) z^{5/6} dz, \quad (3)$$

where γ is the zenith angle and σ_I^2 is measured with an aperture 3 cm in diameter:

$$\sigma_I^2 = \frac{\langle (I(t) - \langle I(t) \rangle)^2 \rangle}{\langle I(t) \rangle^2}. \quad (4)$$

The same expression can also be applied to the index of scintillation which is mainly related to the high-altitude layers of the atmosphere. High-altitude winds are normally blowing from west to east at these latitudes, this is confirmed by the correlation curves in Fig. 3, in which the cross-correlation peaks are at zero coordinate showing that both sites were struck by scintillating layers simultaneously. On the other hand, this corresponds to a correlation coefficient of only 58% which accounts for scintillation related to local turbulence as will be shown in Sec. 3.3.

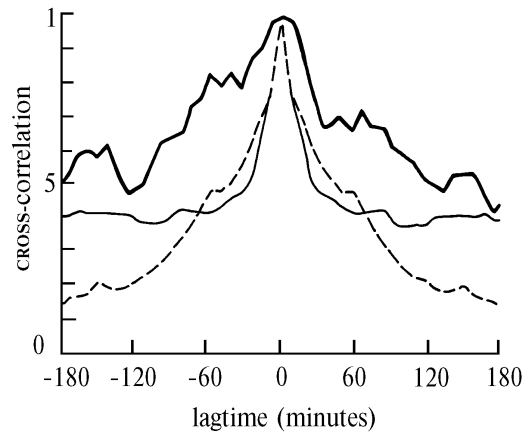


FIG. 3. The temporal correlation of vision quality measurements (the measured interval is 500 sec): Vizcachas autocorrelation (dashed line), Campanas autocorrelation (dotted line), and cross-correlation (solid line).

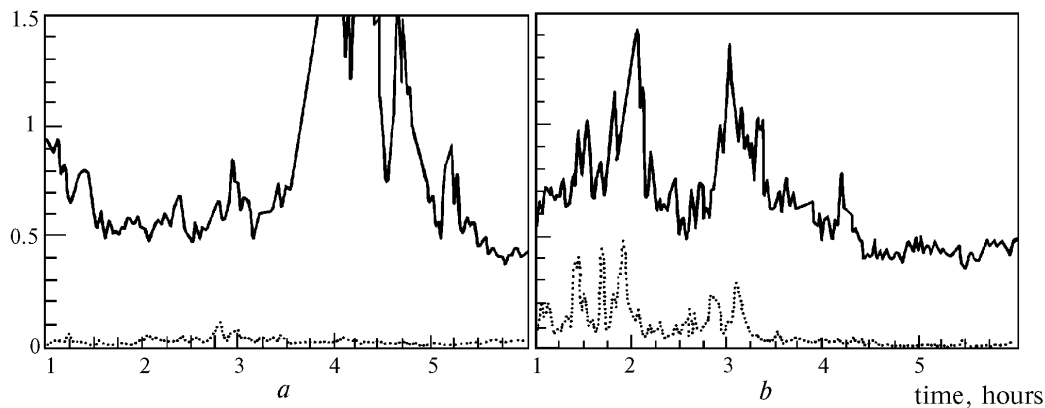


FIG. 4 The vision quality (solid line) and scintillation (dotted line) recorded in Vizcachas (a) and in Las Campanas (b).

3.3. The SODAR as tool for diagnostics and prediction. If the turbulence in the boundary layer has a rather small time constant, one can use the SODAR to predict the turbulence for the time $t + 20$ min from the measurement carried out at time t , provided that one knows the three-dimensional pattern of the wind velocity (see Fig. 4).

The SODAR located at Vizcachas was used in this case to verify the assumption on a conservative turbulence transportation over long distances. We take, for instance, a strong increase in the vision quality which could be attributed to a local effect due to the ground turbulence. As can be seen from Fig. 4, the corresponding SODAR facsimile records show that a very dense layer appeared at 200 m altitude above Vizcachas. Its altitude has been slowly decreasing until complete disappearance. The stronger level of turbulence observed at Vizcachas may be associated with two consecutive bursts of the vision quality recorded at Las Campanas two hours earlier. In this case, the turbulence would have been considerably amplified over the hills on its way from Las Campanas. It is possible, in this particular case, to obtain more information about the behavior of this turbulent layer by more thorough study of the scintillation at both sites as shown in Figs. 4 a and b. It can be seen that the increase in the vision quality over Las Campanas is related to a strong scintillation, which indicates that the turbulence occurred high above the site (possibly 1000–2000 m). On

the contrary, as the SODAR showed, the turbulent layer which reached Vizcachas was at lower altitude and thus could not induce scintillation.

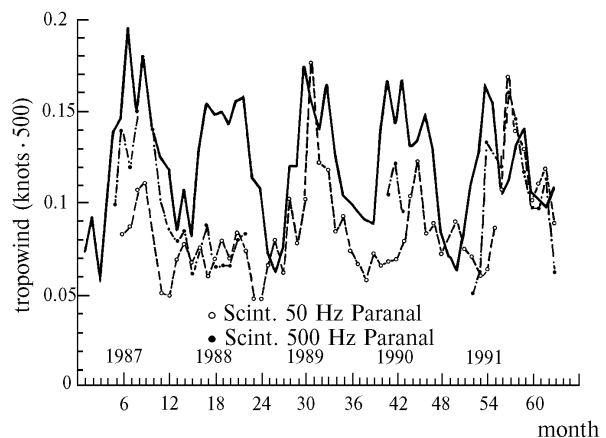


FIG. 5. Comparison of the monthly average value of the wind velocity at the tropopause over Antofagasta (solid line) and the index of scintillation at Cerro Paranal (dashed line) since January 1987.

4. SCINTILLATION AND UPPER-ATMOSPHERIC WIND

4.1. Radiosonde data. In spite of the fact that there is no direct relationships between the wind velocity and thermal turbulence at the ground level we assume that the high wind shear created by the jet stream (where the speed may exceed 60 m/s) increases the probability of appearance of such a relationship. A statistical analysis of the mean wind velocity in the altitude range from 11 to 12 km gives the required information.

Digital files of data on the upper air observations have been purchased from the National Climatic Data Center (NCDC, Asheville, North Carolina, USA). These data are related to meteorological balloons launched twice a day from Lima (Peru), Antofagasta, and Quintero (Santiago) stations during 1958–1984.

4.2. Scintillations. The index of low frequency (< 50 Hz) scintillations is monitored by a DIMM for each of 200 CCD series of 10 ms exposure. The total index of scintillations is measured using the same star at the frequency of 500 Hz with a photomultiplier behind the aperture 3 cm in diameter of a Fabry lens. It is assumed that seasonal variations of the index of scintillations may be indicative of the frequency of occurrence of turbulence in the upper atmosphere. In connection with the current attempts to relate the wind velocity to the refractive index structure,⁶ Fig. 5 shows a comparison of the monthly averaged radiosonde measurements for the

200 mB level over the Chilean Antofagasta station and of the index of scintillations at Paranal (120 km to the south) for the period 1987–1992.

ACKNOWLEDGMENTS.

The data set given in Sec. 3.3 was collected by observers at the VBT site group: R. Castillo, J. Navarrete, and A. Sanchez. We are also indebted to the crew of Las Campanas Observatory for their warm hospitality and, in particular, to E. Cerda, operator of the Carnegie monitor.

REFERENCES

1. A.F. de Baas and M. Sarazin, in: *Abstracts of Papers of the Eighth Symposium on Turbulent Shear Flows*, Munich, September 9–11, 1991.
2. F. Murtagh, M. Sarazin, and H.M. Adorf, in: *Proceeding ESO Conference on Progress in Telescope and Instrumentation Technologies*, edited by M.H. Ulrich, April 27–30, 1992.
3. VLT Site Selection Working Group, VLT Report No. 62, November 14, 1990.
4. M. Sarazin and F. Roddier, *Astron. Astrophys.* **227**, 294–300 (1990).
5. B. Lopez and M. Sarazin, in: *Proceeding ESO Conference on High Resolution Imaging by Interferometry II*, Garching, October 14–18, 1991.
6. C.E. Coulman, J. Vernin, Y. Coqueugniot and J.L. Caccia, *Appl. Opt.* **27**, No. 1, 1988.